

Field-Free Alignment of Molecules Observed with High-Order Harmonic Generation

K. Miyazaki,^{1,*} M. Kaku,¹ G. Miyaji,¹ A. Abdurrouf,² and F. H. M. Faisal²

¹*Institute of Advanced Energy, Kyoto University, Gokasho, Uji, Kyoto 611-0011, Japan*

²*Fakultät für Physik, Universität Bielefeld, D-33615 Bielefeld, Germany*

(Received 22 June 2005; published 8 December 2005)

High-order harmonic generation is demonstrated to provide a sensitive way for an extensive study of dynamic processes in the field-free alignment of strong-field-induced molecular rotational wave packets. The time-dependent harmonic signal observed from field-free-aligned N₂, O₂, and CO₂ has been found to include two sets of beat frequency for pairs of coherently populated rotational states. One of them is the well-known frequency component characterizing the field-free alignment of molecules, and the other is ascribed to the beat that arises from coherence embedded in the wave packet. We discuss the effect of each frequency component on the revival signal observed with the harmonic generation.

DOI: [10.1103/PhysRevLett.95.243903](https://doi.org/10.1103/PhysRevLett.95.243903)

PACS numbers: 42.65.Ky, 33.15.Mt, 33.90.+h

The interaction of an intense ultrashort laser pulse with molecules has theoretically been shown to create a superposition of coherently excited rotational states or a rotational wave packet [1]. This wave packet gives rise to transient alignment of molecules that is recurrent under field-free conditions. There has been much interest in this field-free alignment of molecules, because it provides a promising and versatile way to control molecules with an external field for a variety of applications [2]. The revival structure in the field-free molecular alignment was first observed with the Coulomb explosion imaging by Rosca-Pruna and Vrakking [3]. The fundamental behavior and dynamics of the alignment have been extensively studied so far using the imaging [4,5] and polarization spectroscopy [6,7].

Recently the present authors [8] and Zeidler *et al.* [9] have reported the first observation of high-order harmonic generation (HHG) from the rotational wave packet with an intense femtosecond (fs) laser pulse. In contrast to the HHG from randomly oriented molecules observed so far [10], the harmonic yield was very sensitive to the molecular alignment [11] and strongly modulated by the temporal evolution. The characteristic HHG observed demonstrates an effective approach to an extensive study of wave packet dynamics through the high-order nonlinear optical process [8,9,12–14], while suggesting a possible new area of nonlinear optics using the molecular wave packet to control the strong-field interaction.

The purpose of this Letter is to show a new aspect in the field-free molecular alignment that emerges in the HHG and to discuss the detailed structure and formation process of rotational wave packets in time and frequency domains. We focus our attention on temporal evolutions of harmonic yield from the wave packet in N₂, O₂, and CO₂ and their frequency spectra. The results have shown that the time-dependent harmonic signal includes two sets of beat frequency for pairs of rotational states making up a wave packet. One of them is well known to characterize the field-free alignment of molecules with a full revival period

of $T_{\text{rev}} = 1/(2Bc)$, where B is the rotational constant. The other is ascribed to the beat that results from coherence embedded in the wave packet and creates the revival signal with a period of $T_{\text{rev}}/2$.

We consider a pump-probe experiment for simple linear molecules such as N₂ and O₂, using nonresonant, linearly polarized ultrashort laser pulses. The pump pulse forms a ground-state rotational wave packet $\Psi_g(t) = \sum_J a_J \psi_{JM} \exp(-iE_J t/\hbar)$ that brings about molecular alignment and its field-free revivals, where ψ_{JM} is the field-free rotor wave function, pertaining to the eigenenergy E_J , for the rotational state with the angular momentum J and its projection M on the field direction, and the coefficient a_J depends on the interaction strength and should almost be independent on time after the end of interaction [1]. As theoretically discussed in detail, the degree of alignment is characterized by the expectation value $\langle \cos^2 \theta \rangle$, which is calculated using $\Psi_g(t)$, with the angle θ between the molecular axis and the field direction [1]. It is well known that the time-dependent behavior of $\langle \cos^2 \theta \rangle$ is dominated by beats between any pair of rotational states populated through the transition, $\Delta J \equiv J - J' = 0, \pm 2$ with $\Delta M = 0$. For the rotational states with $E_J = 2\pi\hbar BcJ(J+1)$, the beat frequency is calculated as $\omega_1 = 2\pi Bc(4J+6)$ for a pair of J and $J \pm 2$. This beat usually leads to four transient peaks of $\langle \cos^2 \theta \rangle$ in a revival period $T_{\text{rev}} = 1/(2Bc)$ [3–7].

In the pump-probe experiment, the delayed probe pulse generates high harmonic radiation from the wave packet, and the harmonic signal is observed as a function of time delay Δt between the pump and probe pulses. The HHG from a single molecule is illustrated well by a semiclassical model consisting of three steps of ionization, acceleration of freed electron, and recombination to emit a harmonic photon [15]. This harmonic generation process is essentially a single-cycle event in the laser field. In contrast, the temporal change in the harmonic signal to be observed is very slow and predominantly governed by the beat at ω_1 as for $\langle \cos^2 \theta \rangle$.

The experimental procedure was almost the same as in our recent work [8]. Briefly, the laser can produce pulse energy of 40 mJ in 40 fs pulses at 800 nm. The linearly polarized output was split into two beams to produce a variable time delay Δt between the pump and probe pulses. The two beams were recombined collinearly and focused with a 50 cm focal-length lens into a pulsed molecular beam jetted from a 1 mm diameter nozzle. The gas jet pressure was typically 10 Torr. The accurate time delay of $\Delta t = 0$ was determined by the second-harmonic autocorrelation signal produced with a small portion of the combined pulses. The pump pulse intensity in the gas jet was in a range of $(4-8) \times 10^{13}$ W/cm², while the probe intensity for the HHG was slightly higher than the pump. The harmonic radiation was detected by an electron multiplier mounted on a vacuum ultraviolet monochromator, and the signal processed by a boxcar averager was stored on a personal computer. The probe pulse polarization was fixed to the direction along the monochromator slit, while the pump polarization was usually parallel to the probe and rotated by an angle α if necessary.

In the preliminary experiment we observed the time-dependent signal for all orders of harmonic higher than the 15th for which the semiclassical model [15] would be valid. Since their revival structures represented no fundamental difference, for the present study we selected the 19th harmonic ($\lambda \sim 42.1$ nm) with a good signal to noise ratio.

Figure 1 shows (a) a typical example of the harmonic signal observed for N₂ as a function of Δt and (b) the temporal evolution of $\langle \cos^2\theta \rangle$ simulated under the same pump pulse conditions as in the experiment. The observed time-dependent harmonic signal is well reproduced by the

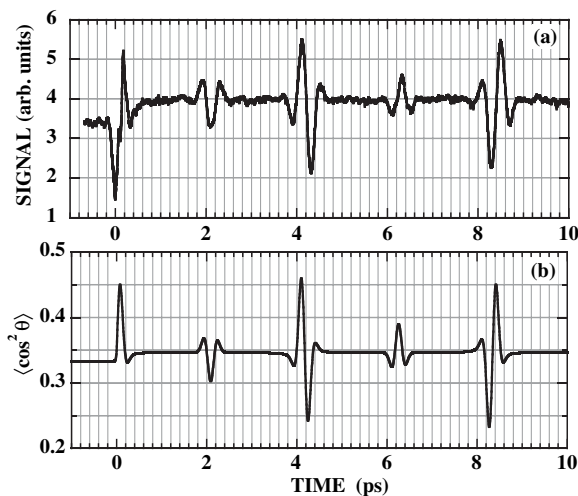


FIG. 1. (a) The 19th harmonic signal observed for N₂ as a function of time delay between the pump and probe pulses at the intensities of 0.8 and 1.7×10^{14} W/cm², respectively, and (b) temporal evolution of $\langle \cos^2\theta \rangle$ simulated under the same pump pulse conditions, where $T_{\text{rot}} = 300$ °K is assumed so as to give the same J value for the peak amplitude as in Fig. 2.

simulated result of $\langle \cos^2\theta \rangle$, except for the signal at $\Delta t \sim 0$. This demonstrates that the harmonic is most efficiently produced with N₂ molecules aligned parallel to the probe pulse field and suppressed with those aligned perpendicularly, as reported so far [8,9,13]. The detailed revival structure is seen comparing the observed signal with the simulated $\langle \cos^2\theta \rangle$. The large signal drop at $\Delta t \sim 0$ is due to strong ionization induced by the high intensity of superimposed pump and probe pulses, which is not taken into account in the simulation. The onset of alignment is shown by the first peak at $\Delta t \sim 0.2$ ps after the pump pulse interaction [16]. This signal peak rapidly decreases due to dephasing of rotational states in the wave packet, but the background signal from randomly oriented molecules is kept higher than that at $\Delta t < 0$. This enhanced background at $\Delta t > 0$ is seen also in the simulated result, whereas $\langle \cos^2\theta \rangle = 1/3$ for the isotropic distribution at $\Delta t < 0$, and attributed to the effect of the time-independent component for $\Delta J = 0$. The full revival of alignment is observed at $\Delta t \sim 8.5$ ps, corresponding to $T_{\text{rev}} = 8.3$ ps with $B = 2$ cm⁻¹ for N₂, where the rapid signal modulation is due to the rotation of aligned molecules.

With the Fourier transform we analyzed the observed time-dependent harmonic signal to see the structure, and the result is shown in Fig. 2. The spectrum is mainly composed of beat frequencies at ω_1 with a separation $\Delta\omega_1/2\pi = 4Bc$, as expected. The spectral amplitude is larger for the even J and weaker for the odd J , representing the intensity alternation that originates from the population ratio 2:1 between the even- and odd- J states of N₂ [17]. Making the inverse Fourier transform for each, we have confirmed that the even- and odd- J states contribute in antiphase to the revival signals at $T_{\text{rev}}/4$ and $3T_{\text{rev}}/4$ to produce the small peak owing to the population difference, as discussed by Dooley *et al.* [4].

The spectrum shown in Fig. 2 includes another set of weak frequency component with a separation of $8Bc$. This

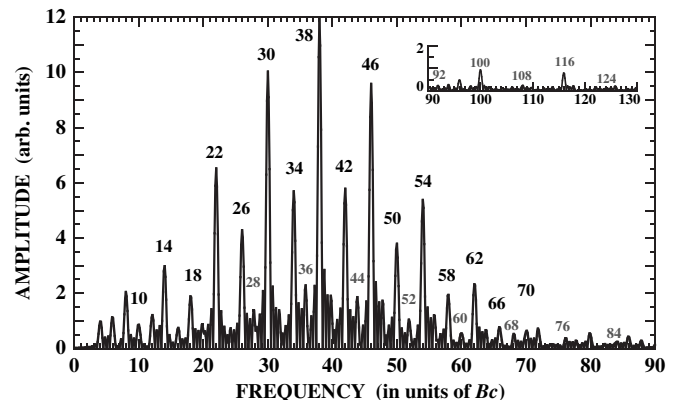


FIG. 2. Frequency spectrum of the time-dependent 19th harmonic signal shown in Fig. 1(a). The inset is the extended spectrum in the higher frequency region. The number on each peak denotes the frequency $4J + 6$ (in black) at ω_1 and $8J + 20$ (in gray) at ω_2 .

component is definitely ascribed to the beat frequency $\omega_2 = (E_{J+4} - E_J)/\hbar = 2\pi Bc(8J + 20)$ for a pair of rotational states J and $J \pm 4$. We note that the rotational wave packet includes such additional coherence as to be detected with the HHG, while $\langle \cos^2\theta \rangle$ is not allowed to contain the ω_2 component due to the selection rule. This coherence between the states for $\Delta J = \pm 4$ would be created by multistep transitions during the wave packet formation process, and then the spectral amplitude at ω_2 should be much weaker than that at ω_1 , as seen in Fig. 2. The time-dependent signal from the ω_2 component is easily shown to have the revival period of $T_{\text{rev}}/2 = 1/(4Bc)$. Since it is difficult to see the effect of the ω_2 component on the revival signal in Fig. 1(a), we discuss it in detail for O_2 .

Figure 3 shows (a) the time-dependent 19th harmonic signal for O_2 and (b) its frequency spectrum. The full revival is seen at $T_{\text{rev}} \sim 11.6$ ps, corresponding to $B = 1.44 \text{ cm}^{-1}$ for O_2 . The revival signals at multiples of $T_{\text{rev}}/4$ represent almost the same amplitude, since only odd- J states are populated in the ground state of O_2 with no nuclear spin. The observed harmonic yield as well as the revival signal was much smaller than that for N_2 . The low HHG efficiency would result from the antisymmetric structure of molecular orbital [18]. We tried to find a different angle α between the pump and probe field directions to produce a larger revival signal, but the best signal modulation was observed at $\alpha \sim 0^\circ$, as well as the highest harmonic yield. This appears to be inconsistent with the previous conclusion [13] that the HHG from aligned O_2 is peaked at $\theta \sim 45^\circ$ and minimized at $\theta \sim 0^\circ$ and 90° , while

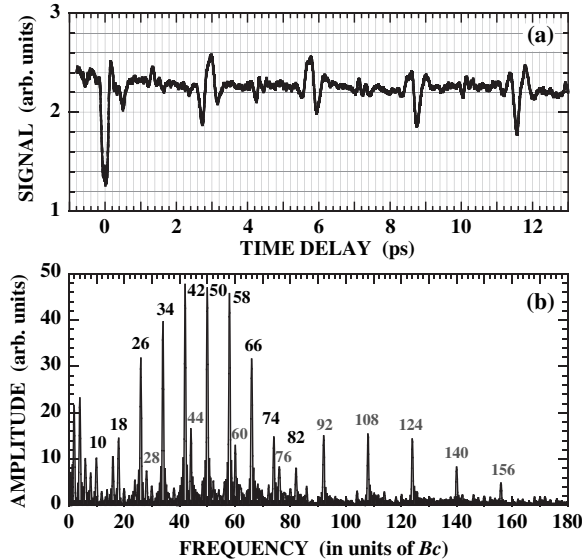


FIG. 3. (a) The 19th harmonic signal observed for O_2 as a function of time delay and (b) its frequency spectrum, in which the number on each spectral peak denotes the frequency $4J + 6$ (in black) at ω_1 and $8J + 20$ (in gray) at ω_2 . The pump and probe pulse intensities are 0.5 and $1.2 \times 10^{14} \text{ W/cm}^2$, respectively.

θ might be different from α , and the phase matching consideration is not involved.

The frequency spectrum shown in Fig. 3(b) consists of the strong component at ω_1 and the weak at ω_2 for only odd J . It is noted that the spectral peaks at $\omega_1/2\pi = (42-58)Bc$ correspond to those at $\omega_2/2\pi = (92-124)Bc$ for almost the same values of $J = 9-13$. This confirms that the ω_2 component certainly originates from the beat between the rotational states J and $J \pm 4$ that are coherently populated in the wave packet.

To see the excitation process to form the wave packet in O_2 , we have simulated the ensemble averages of $\langle \cos^2\theta \rangle$ at different rotational temperatures T_{rot} . The results have shown that the ω_1 component is peaked for $J = 5$ and 11 at $T_{\text{rot}} = 90$ and 300°K , respectively. Since T_{rot} in the supersonic O_2 gas jet would be less than 100°K [19], the spectral peaks for $J = 9-13$ in Fig. 3(b) indicate that the multistep Stokes transitions preferentially take place to shift the initial rotational distribution and form the wave packet, due mainly to the restriction of $\Delta M = 0$ for $|M| \leq J$.

The spectrum shown in Fig. 3(b) appears to involve a different series of the weak ω_2 component at $(28-76)Bc$ with a subpeak for $J = 3$. We believe that this series of the ω_2 in the low frequency region accounts for the initial low temperature T_{rot} in the supersonic gas jet. Our simulation has shown that the spectral peak for $J = 3$ corresponds to $T_{\text{rot}} = 25-50^\circ\text{K}$.

The above discussion on the ω_2 component in the high and low frequency regions is valid also for the N_2 spectrum shown in Fig. 2.

The effect of the ω_2 component on the time-dependent harmonic signal can be seen in Fig. 3(a), where the signal includes weak revival signals at $(2m - 1)T_{\text{rev}}/8$ with positive integer m . The $1/8$ -partial revival signals are shown to arise from the ω_2 component as follows. With the inverse Fourier transform we reconstructed the time-dependent harmonic signal, using one of two components at ω_1 and ω_2 [20]. The results presented in Fig. 4 demonstrate that the ω_1 component certainly creates the revival signals at $mT_{\text{rev}}/4$, while the ω_2 component produces the small revival signals at $mT_{\text{rev}}/8$ with the full revival period of $T_{\text{rev}}/2$. We note that the time-dependent harmonic signal observed is the simple superposition of those arising from two components at ω_1 and ω_2 .

Theoretically, the temporal evolution of $\langle \cos^2\theta \rangle$ does not include the ω_2 component, as discussed above. This suggests that the coherence for the beat at ω_2 is embedded in the wave packet, while detected through the anisotropic electronic response to the linearly polarized probe pulse used for the HHG. The $1/8$ -revival signals for O_2 were also observed so far with the Coulomb explosion imaging [4], where $\langle \cos^2 m\theta \rangle$ was used to analyze the fractional revivals. On the other hand, the analysis with $\langle \sin^2 2\theta \rangle$ was proposed to reproduce the time-dependent harmonic signal for O_2 [13]. The temporal evolution of $\langle \sin^2 2\theta \rangle$ is certainly able to

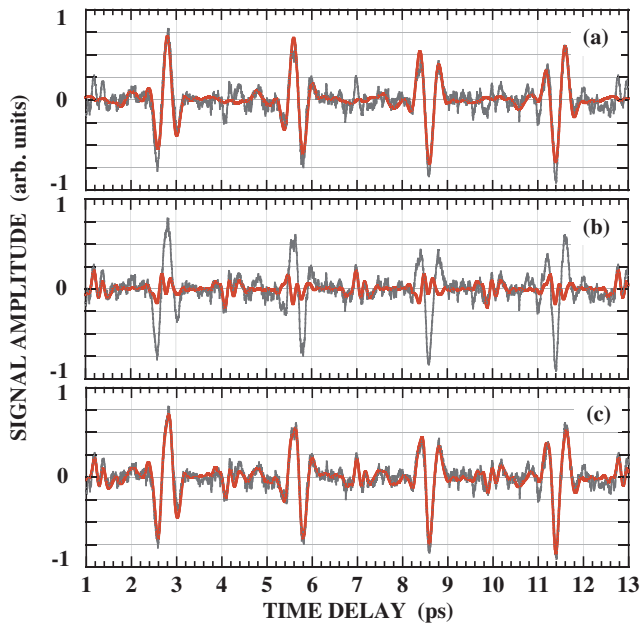


FIG. 4 (color). Time-dependent 19th harmonic signals (red solid lines) reproduced using (a) the frequency component at ω_1 , (b) at ω_2 , and (c) both at ω_1 and ω_2 . For comparison, each trace includes the observed signal given by the gray solid line.

include the ω_2 component that leads to the revival signals at $mT_{\text{rev}}/8$, so that this analysis appears to reconcile with the present picture for the revival signals.

The time-dependent 19th harmonic signal was also measured for CO_2 having only even- J states, where the revival period of 42.7 ps was in good agreement with T_{rev} for $B = 0.39 \text{ cm}^{-1}$, and the frequency spectrum was also observed to consist of the ω_1 and ω_2 components. In contrast to those for N_2 and O_2 , however, the onset of alignment was observed with a signal minimum at $\Delta t \sim 0.3 \text{ ps}$ that was clearly separated from the signal drop at $\Delta t \sim 0$. Corresponding to the first negative peak, the revival signal phase was completely reversed from those in Figs. 1(a) and 3(a). The temporal evolution of $\langle \cos^2 \theta \rangle$ simulated for CO_2 represented the same amplitude phase as those for N_2 and O_2 . These results suggest that the 19th harmonic is minimized with CO_2 aligned along the pump pulse polarization and peaked with those aligned perpendicularly. This might be induced by the destructive interference of recombining electron wave [21,22] and/or by the θ -dependent HHG process characteristic to CO_2 molecules. The experimental results on the harmonic signal phase will be presented and discussed in a separate paper.

In summary, the results of time-dependent HHG from rotational wave packets and its frequency analysis have shown a new aspect in the revival structure of field-free molecular alignment. The present results are useful for controlling rotational wave packets with ultrashort laser pulses [23] and nonlinear optical processes in molecules.

*Electronic address: miyazaki@iae.kyoto-u.ac.jp

- [1] J. Ortigoso *et al.*, J. Chem. Phys. **110**, 3870 (1999); T. Seideman, Phys. Rev. Lett. **83**, 4971 (1999); J. Chem. Phys. **115**, 5965 (2001); L. Cai, J. Marango, and B. Friedrich, Phys. Rev. Lett. **86**, 775 (2001); M. Machholm, J. Chem. Phys. **115**, 10724 (2001).
- [2] H. Stapelfeldt and T. Seideman, Rev. Mod. Phys. **75**, 543 (2003), and references therein.
- [3] F. Rosca-Pruna and M. J. J. Vrakking, Phys. Rev. Lett. **87**, 153902 (2001); J. Chem. Phys. **116**, 6567 (2002); **116**, 6579 (2002).
- [4] P. W. Dooley *et al.*, Phys. Rev. A **68**, 023406 (2003).
- [5] I. V. Litvinyuk *et al.*, Phys. Rev. Lett. **90**, 233003 (2003).
- [6] M. Comstock, V. V. Lozovoy, and M. Dantus, Chem. Phys. Lett. **372**, 739 (2003).
- [7] V. Renard *et al.*, Phys. Rev. Lett. **90**, 153601 (2003); Phys. Rev. A **70**, 033420 (2004).
- [8] M. Kaku, K. Masuda, and K. Miyazaki, Jpn. J. Appl. Phys. **43**, L591 (2004).
- [9] D. Zeidler *et al.*, in *Ultrafast Optics IV*, edited by F. Krausz *et al.* (Springer, New York, 2004), p. 247.
- [10] H. Sakai and K. Miyazaki, Appl. Phys. B **61**, 493 (1995); Y. Liang *et al.*, J. Phys. B **27**, 5119 (1994).
- [11] R. Velotta, N. Hay, M. B. Mason, M. Castillejo, and J. P. Marangos, Phys. Rev. Lett. **87**, 183901 (2001); N. Hay *et al.*, Phys. Rev. A **65**, 053805 (2002).
- [12] J. Itatani *et al.*, Nature (London) **432**, 867 (2004).
- [13] J. Itatani *et al.*, Phys. Rev. Lett. **94**, 123902 (2005).
- [14] K. Miyazaki *et al.*, in *Ultrafast Phenomena XIV*, edited by T. Kobayashi *et al.* (Springer, New York, 2005), p. 195.
- [15] P. B. Corkum, Phys. Rev. Lett. **71**, 1994 (1993).
- [16] K. Miyazaki, T. Shimizu, and D. Normand, J. Phys. B **37**, 753 (2004).
- [17] G. Herzberg, *Molecular Spectra and Molecular Structure, I. Spectra of Diatomic Molecules* (Van Nostrand Reinhold, New York, 1950), Chap. III.
- [18] A. Jarón-Becker, A. Becker, and F. H. M. Faisal, Phys. Rev. A **69**, 023410 (2004); B. Shan, X. M. Tong, Z. Zhao, Z. Chang, and C. D. Lin, Phys. Rev. A **66**, 061401(R) (2002).
- [19] A. Owyong, R. A. Hill, and P. Esherick, Opt. Lett. **8**, 425 (1983).
- [20] For the inverse Fourier transform, we ignored the low frequency components less than 0.6 THz, because the time-dependent second-harmonic autocorrelation signal has shown that such components came from the fluctuation of the laser output.
- [21] M. Lein, N. Hay, R. Velotta, J. P. Marangos, and P. L. Knight, Phys. Rev. A **66**, 023805 (2002); R. de Nalda *et al.*, Phys. Rev. A **69**, 031804(R) (2004).
- [22] T. Kanai, S. Minemoto, and H. Sakai, Nature (London) **435**, 470 (2005).
- [23] M. Spanner, E. A. Shapiro, and M. Ivanov, Phys. Rev. Lett. **92**, 093001 (2004); C. Z. Bisgaard, M. D. Poulsen, E. Peronne, S. S. Viftrup, and H. Stapelfeldt, Phys. Rev. Lett. **92**, 173004 (2004); K. F. Lee, D. M. Villeneuve, P. B. Corkum, and E. A. Shapiro, Phys. Rev. Lett. **93**, 233601 (2004).